Fatigue resistant lead-free multilayer ceramic capacitors with ultrahigh energy density

WANG, Ge, LU, Zhilun, YANG, huijing, JI, hongfen, MOSTAED, Ali, LI, linhao, WEI, yiqi, FETEIRA, Antonio <http://orcid.org/0000-0001-8151-7009>, SUN, Shikuan, WANG, Dawei, SINCLAIR, Derek and REANEY, Ian M

Electronic Supplementary Information

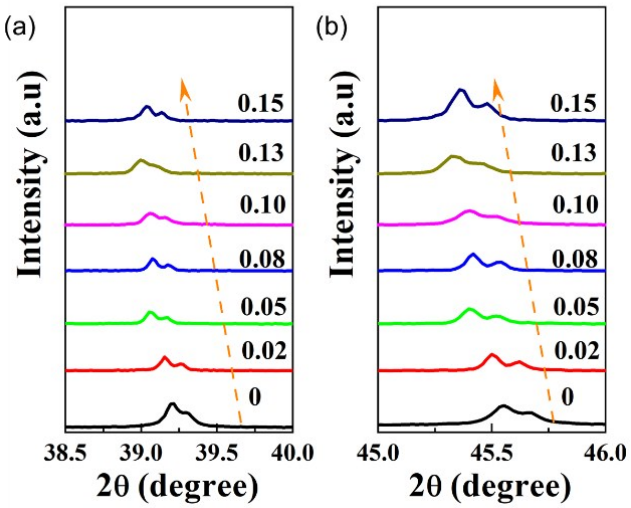

Figure S1. Representative diffraction peaks of (a) $\{111\}_p$ and (b) $\{200\}_p$ for all composition in BF-BT-xBLN ceramics.

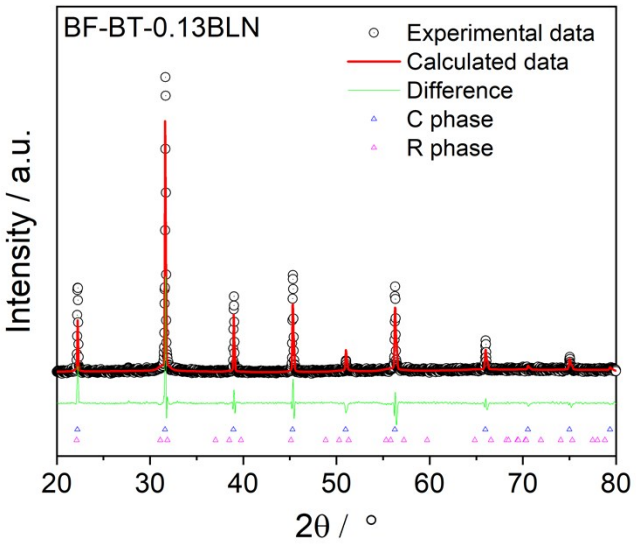

Figure S2 Full-pattern refinement data for BF-BT-0.13BLN ceramic using mixed-phase of *R3c* rhombohedral and *Pm3m* Cubic.

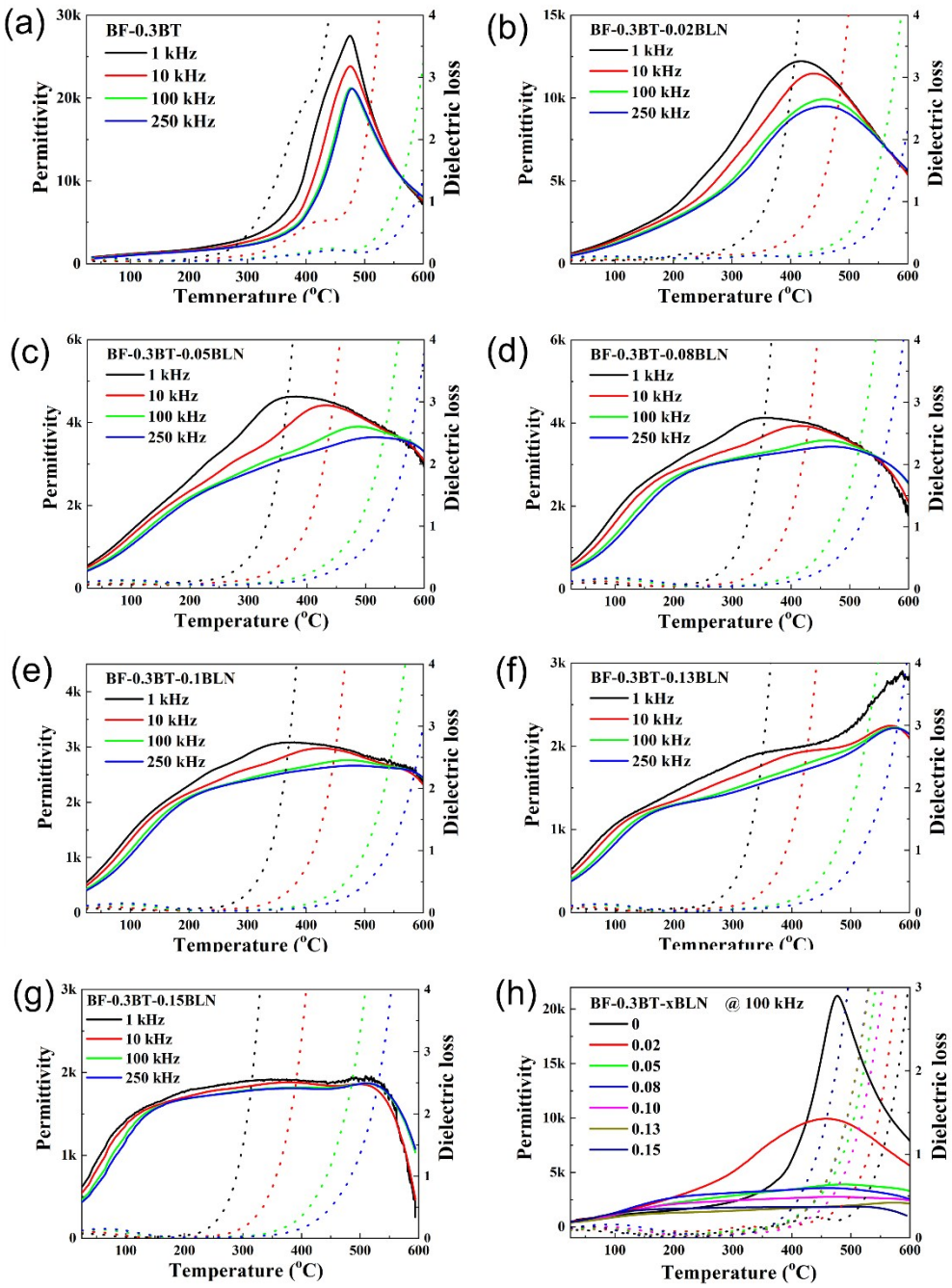

Figure S3. (a-g) Temperature-dependent permittivity and dielectric loss data at a frequency of 1, 10, 100 and 250 kHz for BF-0.3BT-xBLN ceramics. (h) Temperature-dependent permittivity and dielectric loss data for BF-BT-xBLN ceramics at 100 kHz.

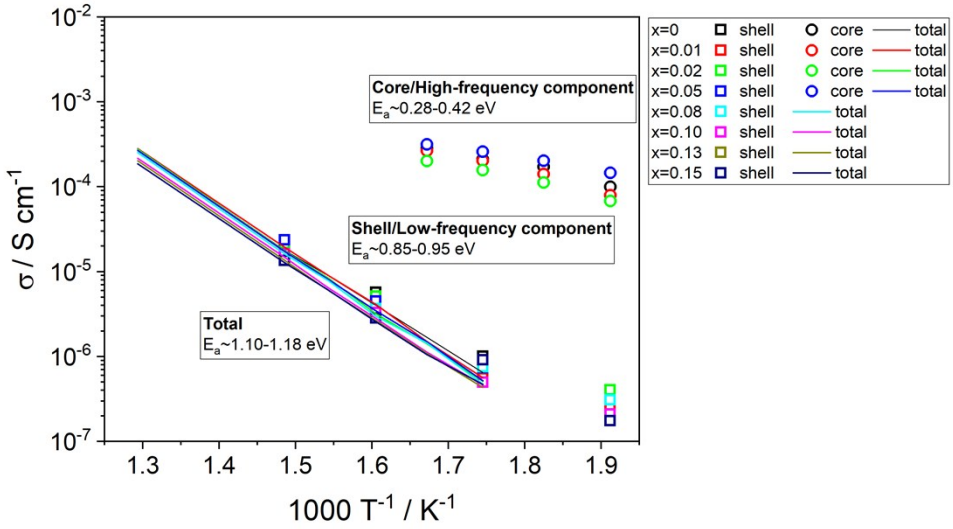

Figure S4. Arrhenius plots of core, shell and total conductivity values for BF-BT-xBLN ceramics.

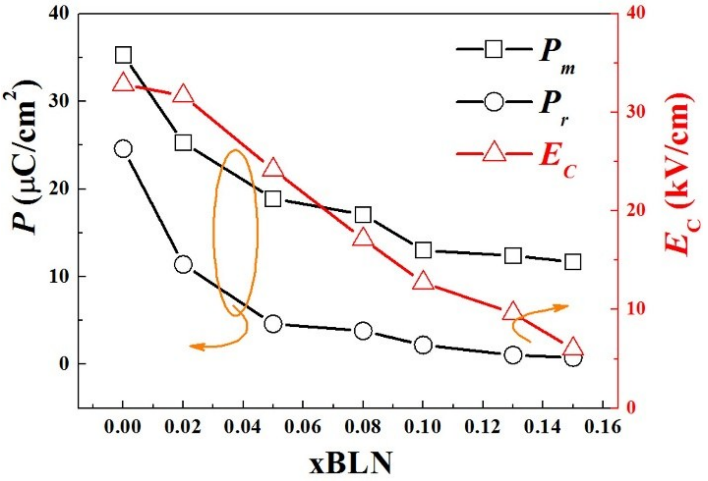

Figure S5. Changes of P_m, P_r and E_c for BF-BT-xBLN ceramics

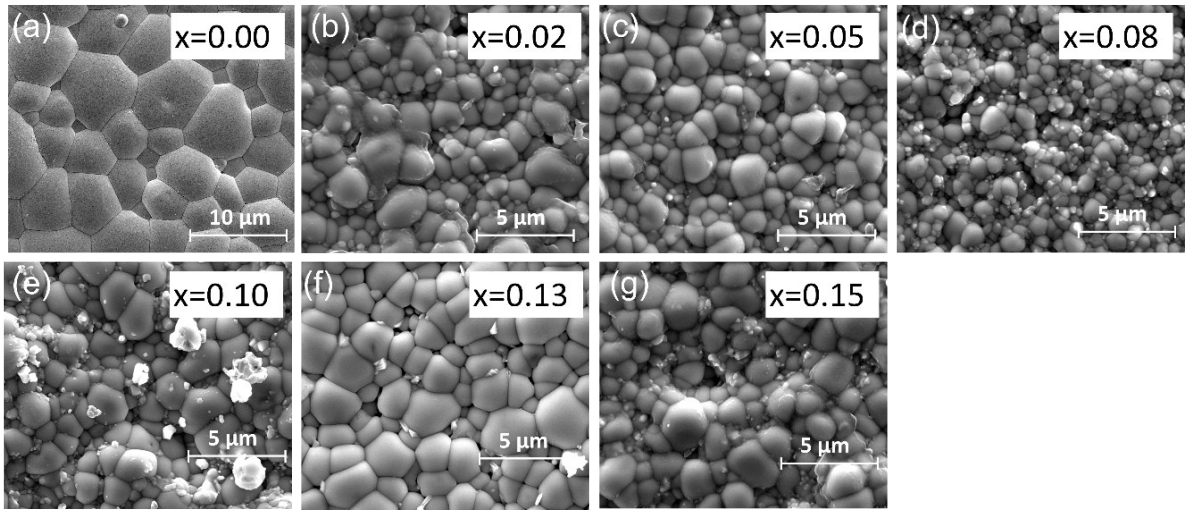

Figure S6 SEM surface micrographs for BF-BT-xBLN (x=0.00-0.15) ceramics.

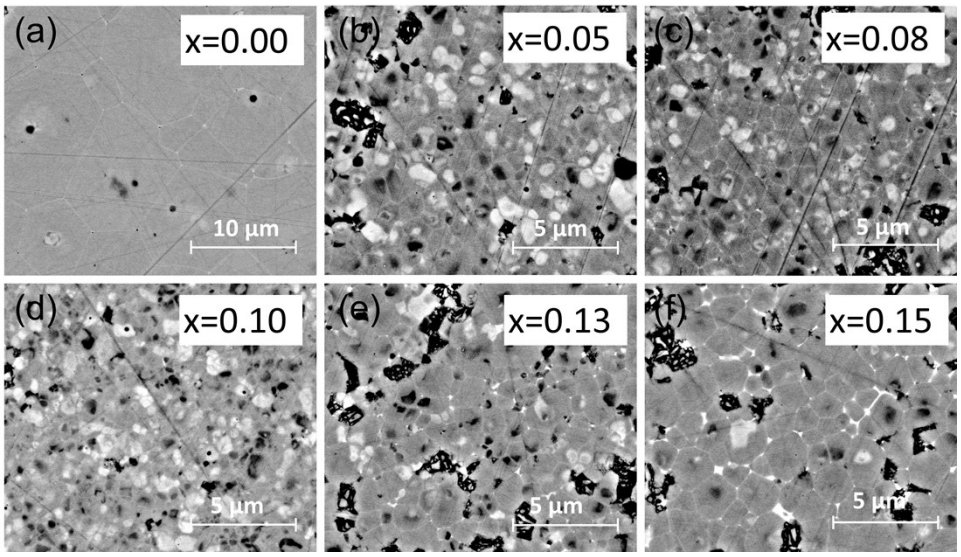

Figure S7 BSE micrographs of polished surfaces for BF-BT-xBLN (x=0.00-0.15) ceramics.

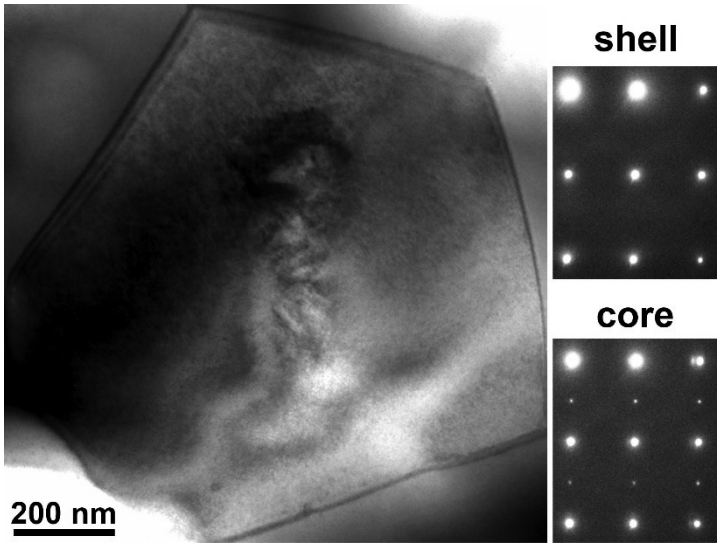

Figure S8. TEM domain morphology with diffraction spots for BF-BT-0.13BLN ceramics.

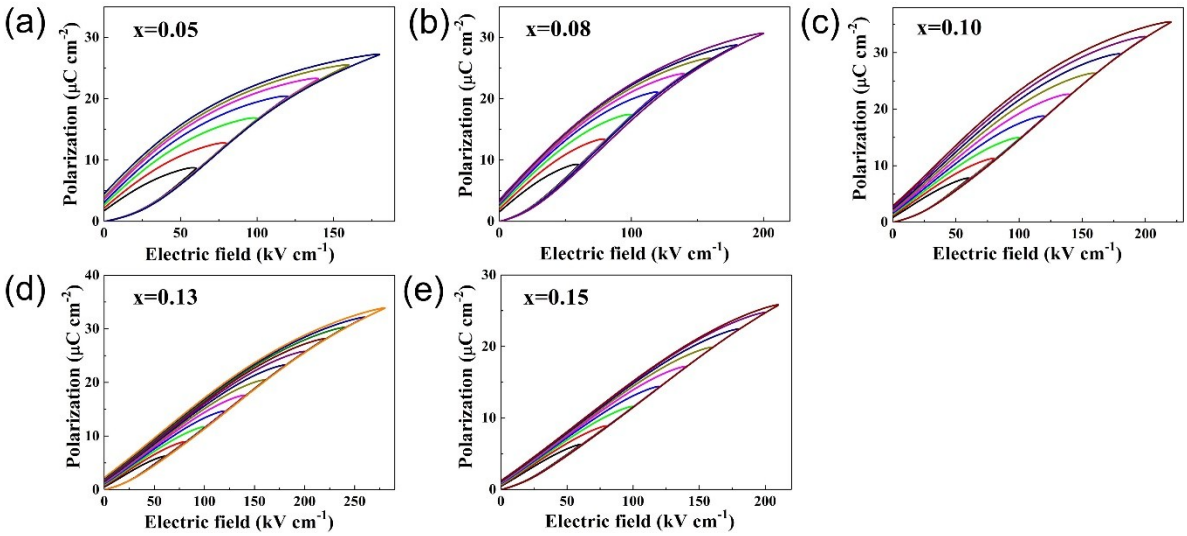

Figure S9. Unipolar P-E loops up to E_{max} for BF-BT-xBLN ceramics.

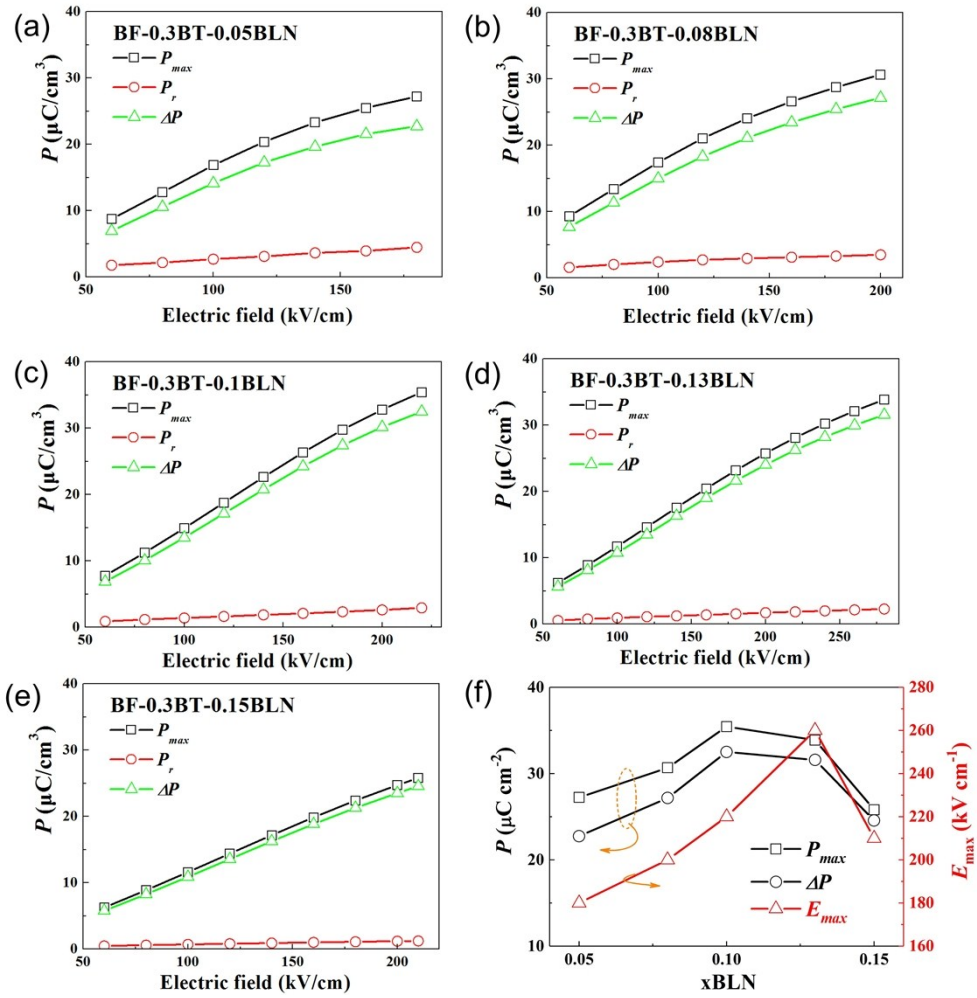

Figure S10. (a-e) P_{max}, P_r and ΔP versus electric field for BF-0.3BT-xBLN ceramics. (f) Changes of P_{max}, ΔP and E_{max} as function of BLN concentration.

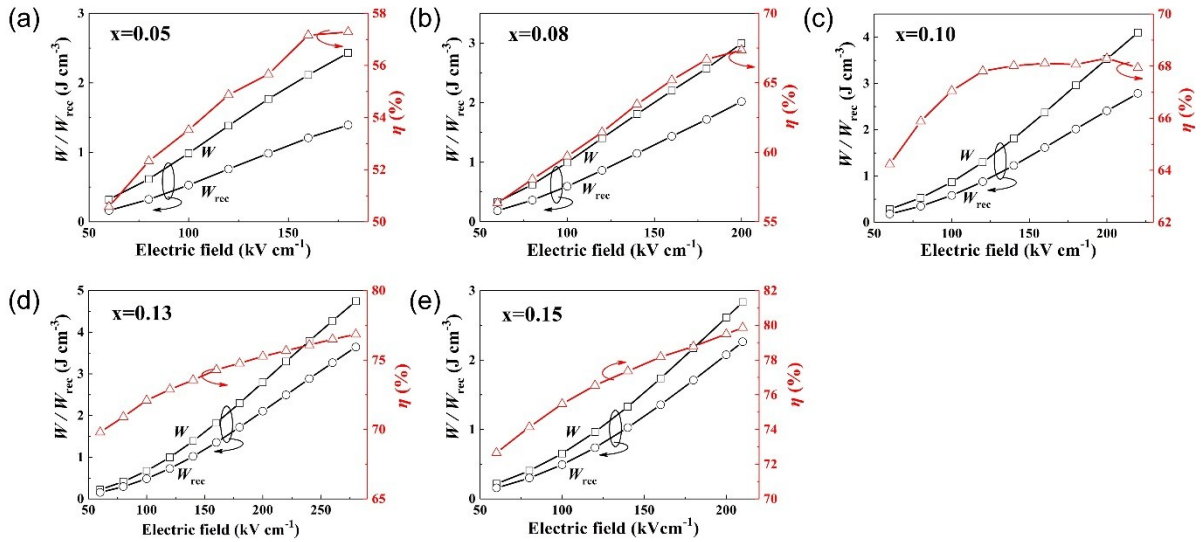

Figure S11. (a-e) W, W_{rec} and η at different electric fields for BF-BT-xBLN ceramics.

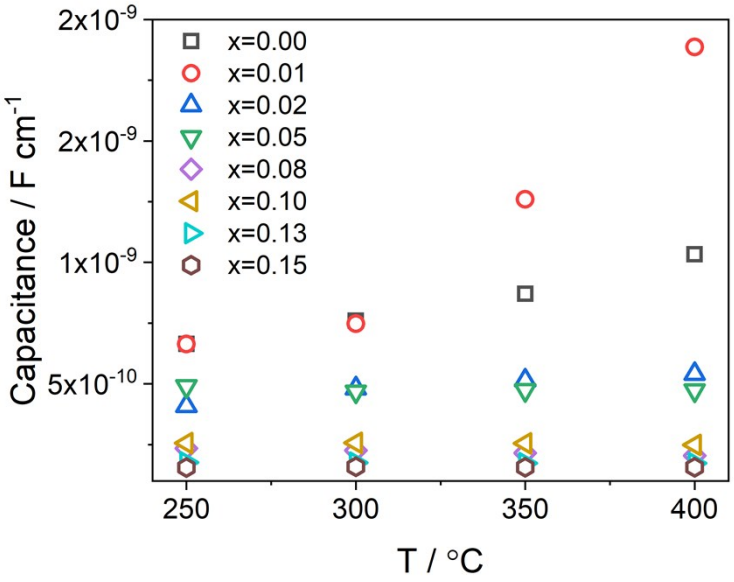

Figure S12. Variation in capacitance associated with the dominant M'' peak in the M'' spectra for BF-BT-xBLN ceramics in the temperature range ~ 250 to 400 °C.

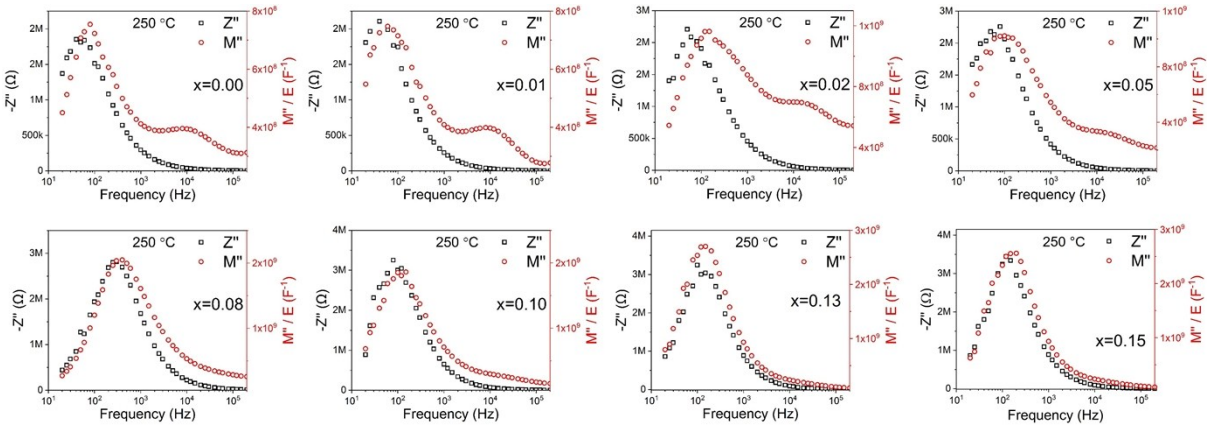

Figure S13. Combined Z'' and M'' spectroscopic plots at 250 °C for BF-BT-xBLN ceramics.

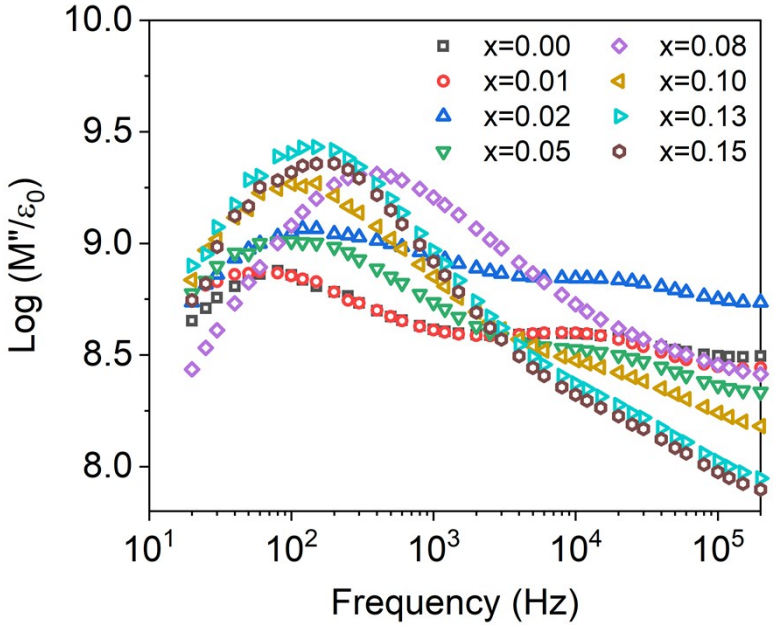

Figure S14. Log M'' verses log f plots at 250 °C for BF-BT-xBLN ceramics.

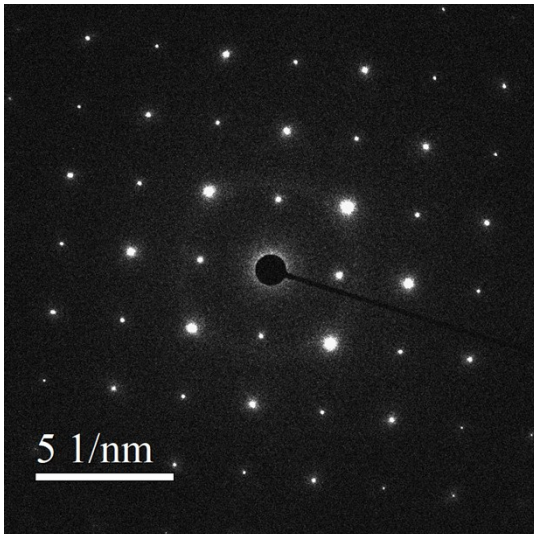

Figure S15. <100> SAD pattern obtained from the BF-BT-13BLN ceramic.

Composition	Space group	Lattice parameter			Phase fraction / %	R_{wp}	GOF
		a / Å	b / Å	c / Å			
BF-BT-0.13BLN	*R3c*	5.6316(7)	5.6316(7)	13.9806(2)	13.6	7.85	1.86
	Pm3m	4.0305(10)	4.0305(12)	4.0305(7)	86.4		

Table S1. Refined structural parameters for BF-BT-0.13BLN ceramics. *GOF: goodness of fitting

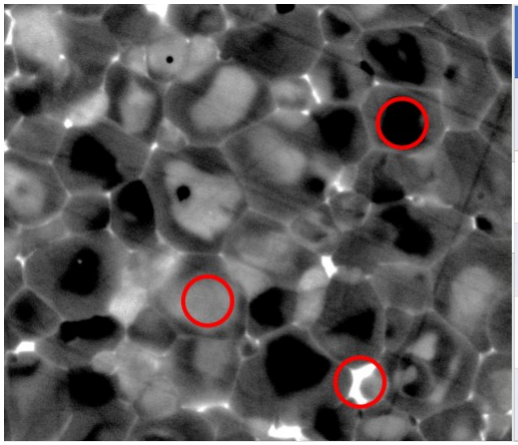

	GB bright	White	Dark	Overall
Bi	33.8%	20.5%	13.2%	16.1%
Fe	3.5%	15.8%	8.9%	12.5%
Ba	1.9%	4.4%	8.7%	6.9%
Ti	2.2%	5.1%	9.1%	6.5%
Results	Bi-rich	Bi/Fe-rich	Ba/Ti-rich	N/A

Table S2. Atomic percentage (excl. O) of BF-BT-0.13BLN quantified from EDS spectra from the ringed regions.

Materials	**W_{rec} / J cm^{-3}**	**η / %**	**ref**
BT-BLT	2.2	89	19
NBT-SBT	9.5	92	31
Nd-BF-BT	6.74	77	40
BF-BT-NZZ	10.5	87	45
BT-BZNT	8.13	95	23
BT-BZNT	10.12	89	22
Ba, Zr-PLZT	6.8	61.2	70
BT-BLN	4.5	92	21
BT-BS	6.1	N/A	71

Table S3. W_{rec} vs. η for different lead-free multilayers